

## Supplementary Information

### **Waterborne-Reduced Graphene Oxide Dispersed Bio-Polyester amide Nanocomposites: An Approach towards Eco-Friendly Anticorrosive coatings.**

Mohd Irfan<sup>1</sup>, Shahidul Islam Bhat<sup>1</sup> and Sharif Ahmad<sup>1\*</sup>

1. Materials Research Laboratory, Department of Chemistry, Jamia Millia Islamia New  
Delhi, India-110025.

Corresponding author. E-mail: sharifahmad\_jmi@yahoo.co.in

#### **Cover Sheet**

<b>1. Total number of Pages:</b>	<b>S1-15 (15 Pages)</b>
<b>2. Total number of Figures:</b>	<b>13</b>
<b>3. Total number of tables</b>	<b>3</b>
<b>4. Total number of Schemes</b>	<b>1</b>

## Characterization

The structural characterizations of the synthesized GO, RGO, WBPEA, WBPEA-PMF-80 and WBPEA-PMF-80-RGO-x were carried out with the help of FT-IR and NMR ( $^1\text{H}$  and  $^{13}\text{C}$ ) spectroscopies. The FT-IR spectra of these materials were taken using IR Affinity-I model Shimadzu on ZnSe cell over a range of  $400\text{--}4000\text{ cm}^{-1}$ . The structural elucidation of WBPEA and WBPEA-PMF-80 were performed by NMR spectroscopy using Bruker Advance III 500 MHz NMR in  $\text{CDCl}_3$  and TMS as the internal standard. The diffraction pattern analysis of GO and RGO was conducted by XRD spectrophotometer (Rigaku Rotaflex (RU-200B)), while the defect/disorder and size of RGO was analyzed by Raman spectrometer (STR 150 series, Japan) which confirmed the reported nano size structure of GO and RGO crystal lattice along with their functionalization. The physico-chemical (acid value, refractive index, specific gravity, solubility, viscosity) and Physico-mechanical properties impact resistance [ASTM D 2794-93], (scratch hardness [ASTM D 1474-98], bending test [ASTM-D522-93a], cross-hatch test (ASTM D3359) and methyl ethyl ketone (MEK) solvent rub test (ASTM D5402) of WBPEA-PMF-80 and WBPEA-PMF-80-RGO-x coatings were conducted.<sup>1</sup> The coating thickness was measured by Elcometer (ASTM B 499 Model 345 Elcometer instrument, Manchester, UK). The morphology of corroded and uncorroded coated CS with WBPEA-PMF-80 and WBPEA-PMF-80-RGO-x was investigated by field-emission scanning electron microscopy (FE-SEM, ZEISS Ultra 55, Germany), while the dispersion pattern of RGO nanofiller in the WBPEA matrix was studied by Transmission electron microscopy (TEM FEI Technai F30, Holland). The optical micrographs of cross hatched WBPEA-PMF-80 and WBPEA-PMF-80-RGO-x coated CS were taken on Lietz Optical Microscope (Model Metallux-3). The thermal stability of these coatings were performed by using thermogravimetric analyser (NETZSCH; STA 449 F1 Jupiter). 3-8 mg of fine powder sample was prepared and loaded on the sample pan (made

up of platinum) under nitrogen atmosphere with a purging flow rate of 40 mL/min. The sample was heated at a heating rate of 10 °C min<sup>-1</sup> in the temperature range of 30°C-800°C.

Electrochemical corrosion studies of coated and bare CS were performed with the help of a conventional three electrode system (viz Ag/AgCl as the reference electrode, test specimen and the platinum gauze as the working and the auxiliary electrodes,) using EG&G glass cell of 400 mL capacity. The working electrode (1.0 cm<sup>2</sup>) area of which was exposed to the solution using a Potentiodynamic/Galvanostat micro Autolab type III (3AVT 70762, The Netherlands) in the pH solutions of pH 4, 7 and 9.2 at 30°C. Prior to all electrochemical testing, the working electrode was allowed to stabilize for a period of 15 minutes, then its open circuit potential (OCP) was recorded for a period of 600 s as a function of time. After OCP stabilization, impedance measurements were made at respective corrosion potentials ( $E_{corr}$ ) over the frequency range (100 kHz to 0.1 Hz), with a signal amplitude perturbation of 10 mV under different corrosive media. The PDP tests were carried out at a scan rate 0.001 mV s<sup>-1</sup> in the potential range of ±100 mV. The impedance and Tafel parameters were determined with the help of a curve fitting programme available in the Nova 1.10 software. Each test was made to run in triplicate to verify the reproducibility of the data. The polarization resistance ( $R_p$ ) of the bare and coated CS was evaluated with the help of Tafel plots using Stearn-Geary equation given in equation (1).

$$R_p = \frac{\beta_a \beta_c}{2.303(\beta_a + \beta_c)i_{corr}} \quad (1)$$

The intersection of the linear anodic and cathodic curves,  $\beta_a$  and  $\beta_c$  and cathodic Tafel slopes give the value of corrosion current density ( $i_{corr}$ ).

The salt spray test (ASTM D 1654) on WBPEA-PMF-80 and WBPEA-PMF-80-RGO-x coatings was carried out for 15 days (360 h) in a salt mist chamber. The salt chamber was

heated at 35°C and the saline fog (5% NaCl solution) was introduced in presence of 90% humidity. The morphology of the corroded surface of WBPEA-PMF-80 and WBPEA-PMF-80-RGO-1.5 coatings after salt spray test was analyzed with help of SEM micrographs, recorded on HR-SEM model SIGMA at the Centre for Nanoscience and Nanotechnology, Jamia Millia Islamia New Delhi India.

### **Biodegradability studies**

The biodegradability tests of WBPEA-PMF-80 and their nanocomposite (WBPEA-PMF-80-RGO-0.5, WBPEA-PMF-80-RGO-1.0 and WBPEA-PMF-80-RGO-1.5) was conducted for a period of 28 days (Fig. S13). The samples were placed in a beaker containing soil with over 30% humidity. The sample of standard size (1cm×1cm) were taken in separate beakers, the mass loss (Fig. S13) after the degradation of these samples in soil were measured with the help of an analytical balance (with accuracy  $\pm 0.0001$ ) for period of 28 days. The graphs between weight loss Vs. time revealed that the high weight loss observed in case of WBPEA-PMF-80 as compared to that of WBPEA-PMF-80-RGO-0.5, WBPEA-PMF-80-RGO-1.0 and WBPEA-PMF-80-RGO-1.5. The WBPEA-PMF-80 started to degrade after 7 days of incubation, while WBPEA-PMF-80-RGO-0.5 began to degrade after 14 days and WBPEA-PMF-80-RGO-1.0 start degrading after 21 days. The sluggish degradation rate was observed in case of WBPEA-PMF-80-RGO-1.5 even after 28 days, which can be attributed to the higher loading of RGO. Moreover, the chemical and electrostatic interactions between polar functionalities of polymer matrix and RGO nanofiller also lead to slow degradation in case of nanocomposites.<sup>2</sup>



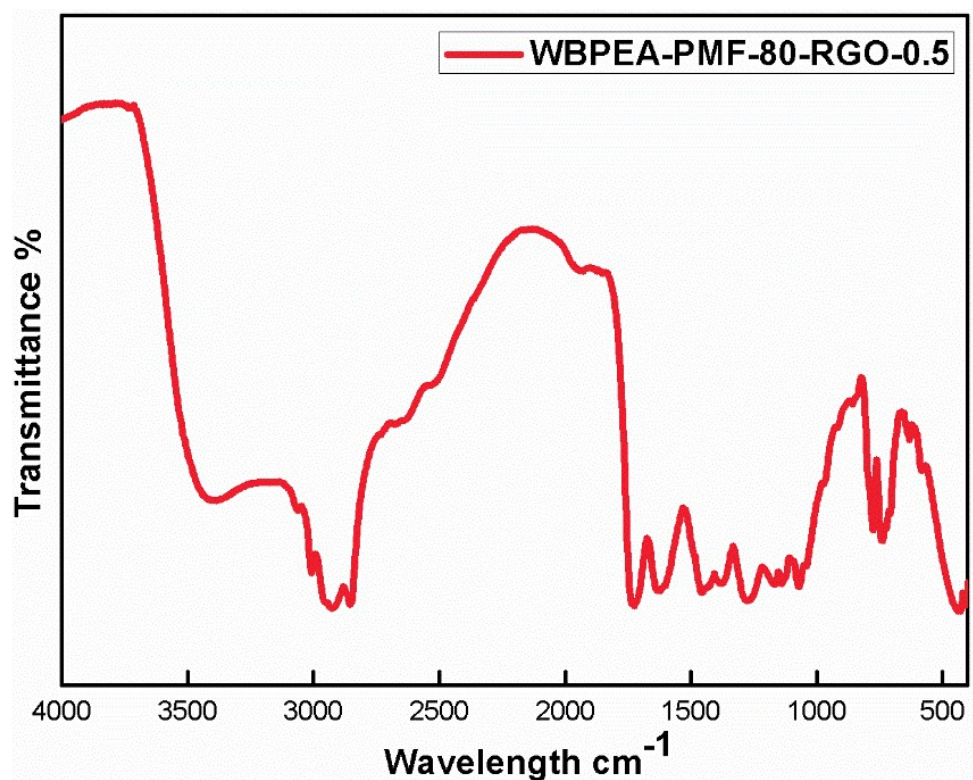


Fig. S2. FTIR spectra of WBPEA-PMF-RGO-0.5

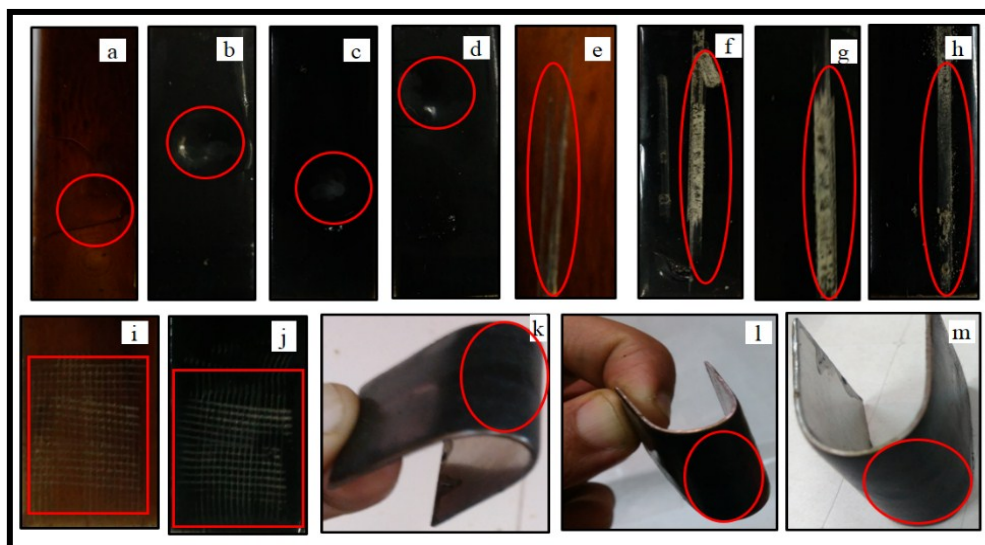
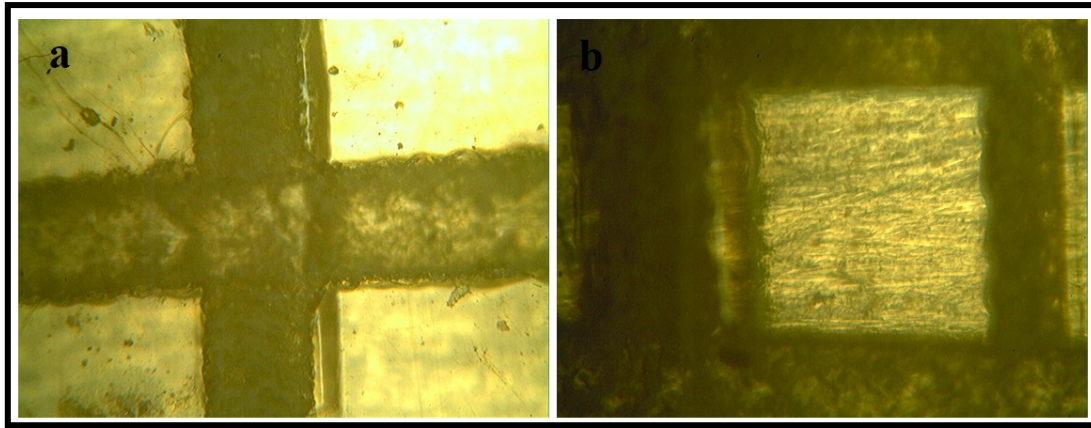
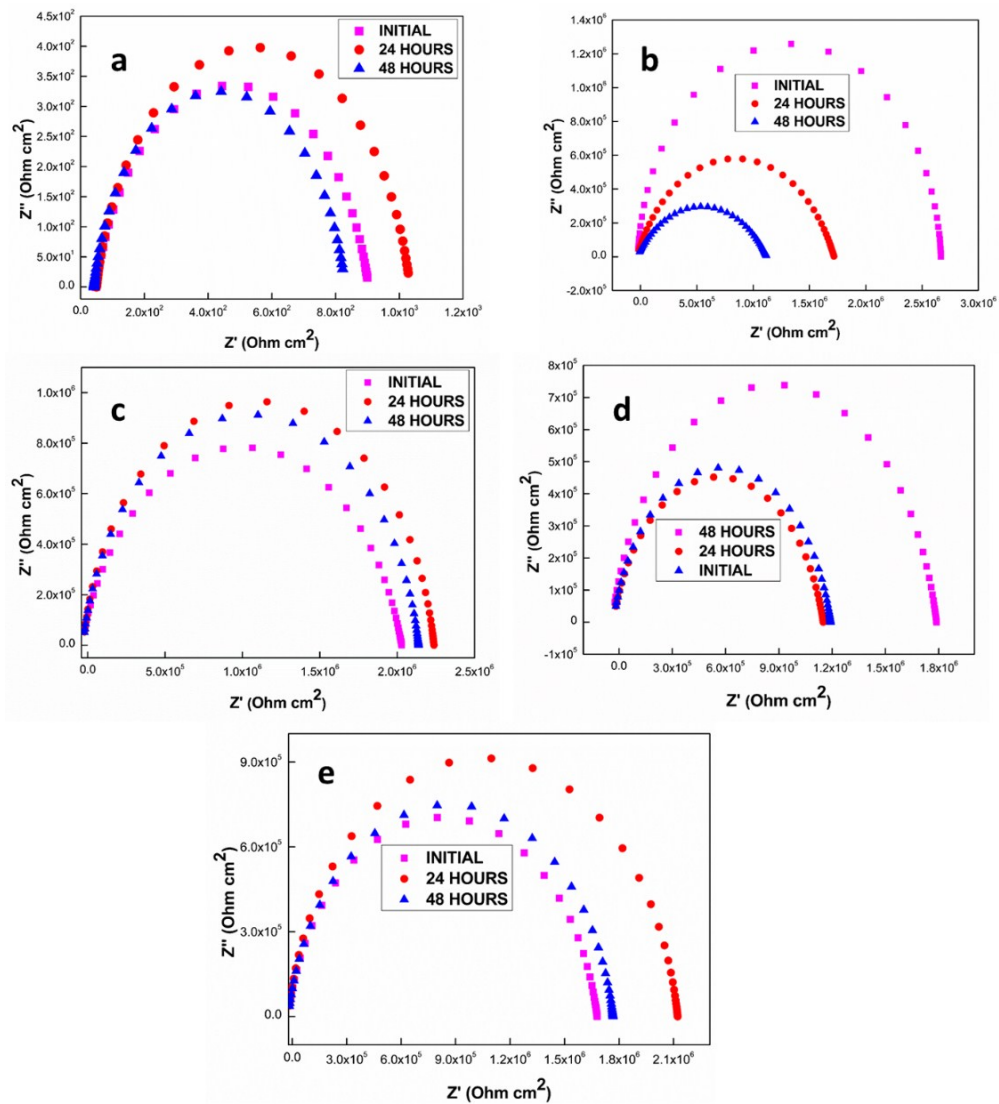


Fig. S3. Digital images of coatings after physico-mechanical test.



**Fig. S4.** Cross-hatch adhesion test (a) WBPEA-PMF-80 (b) WBPEA-PMF-80-RGO-0.5.



**Fig. S5.** Nyquist plots in pH 4 (a) bare CS (b) WBPEA-PMF-80 (c) WBPEA-PMF-80-RGO-0.5 (d) WBPEA-PMF-80-RGO-1.0 (e) WBPEA-PMF-80-RGO-1.5.

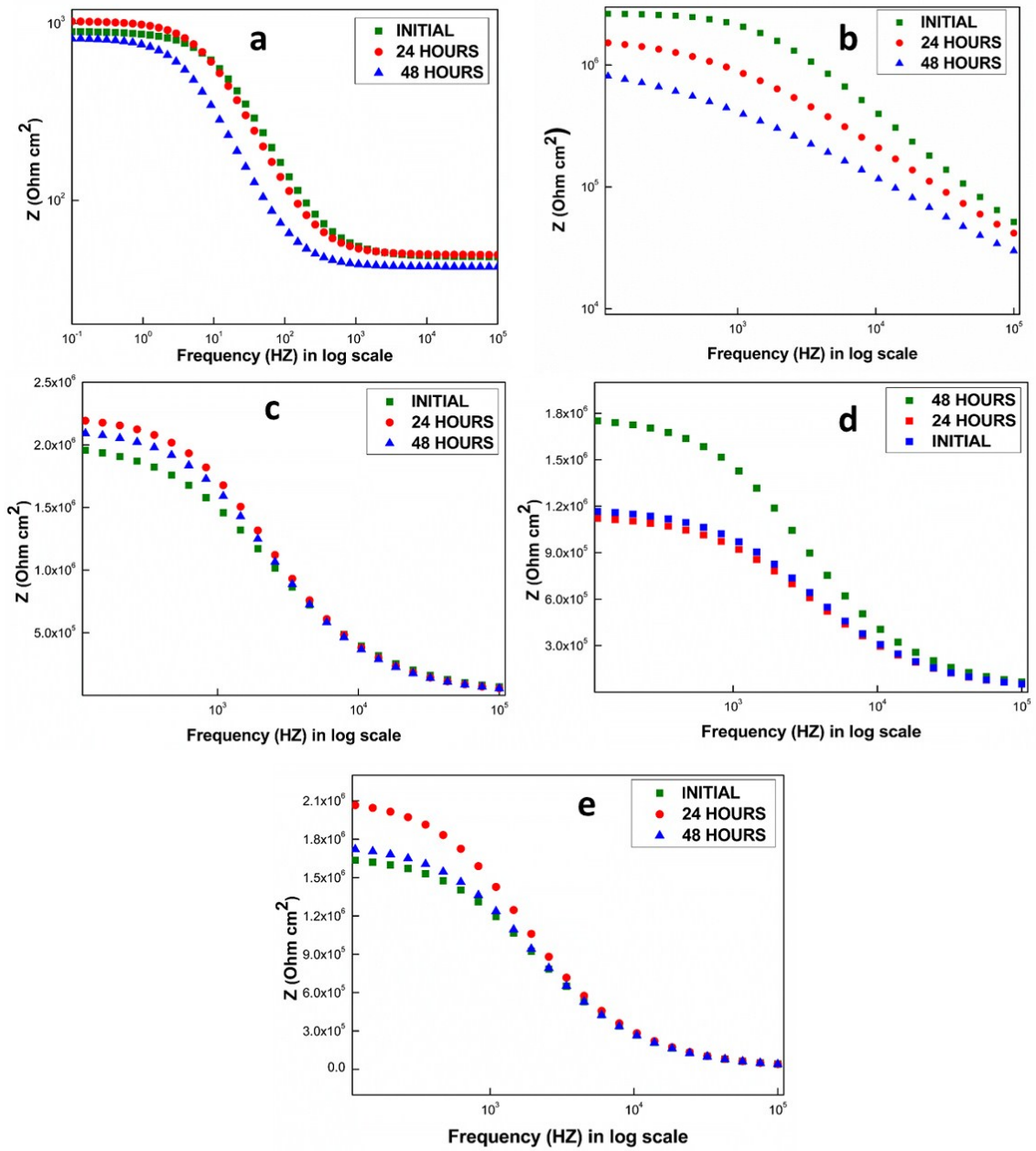


**Fig. S6.** Bode plots in pH 4 (a) bare CS (b) WBPEA-PMF-80 (c) WBPEA-PMF-80-RGO-0.5 (d) WBPEA-PMF-80-RGO-1.0 (e) WBPEA-PMF-80-RGO-1.5.

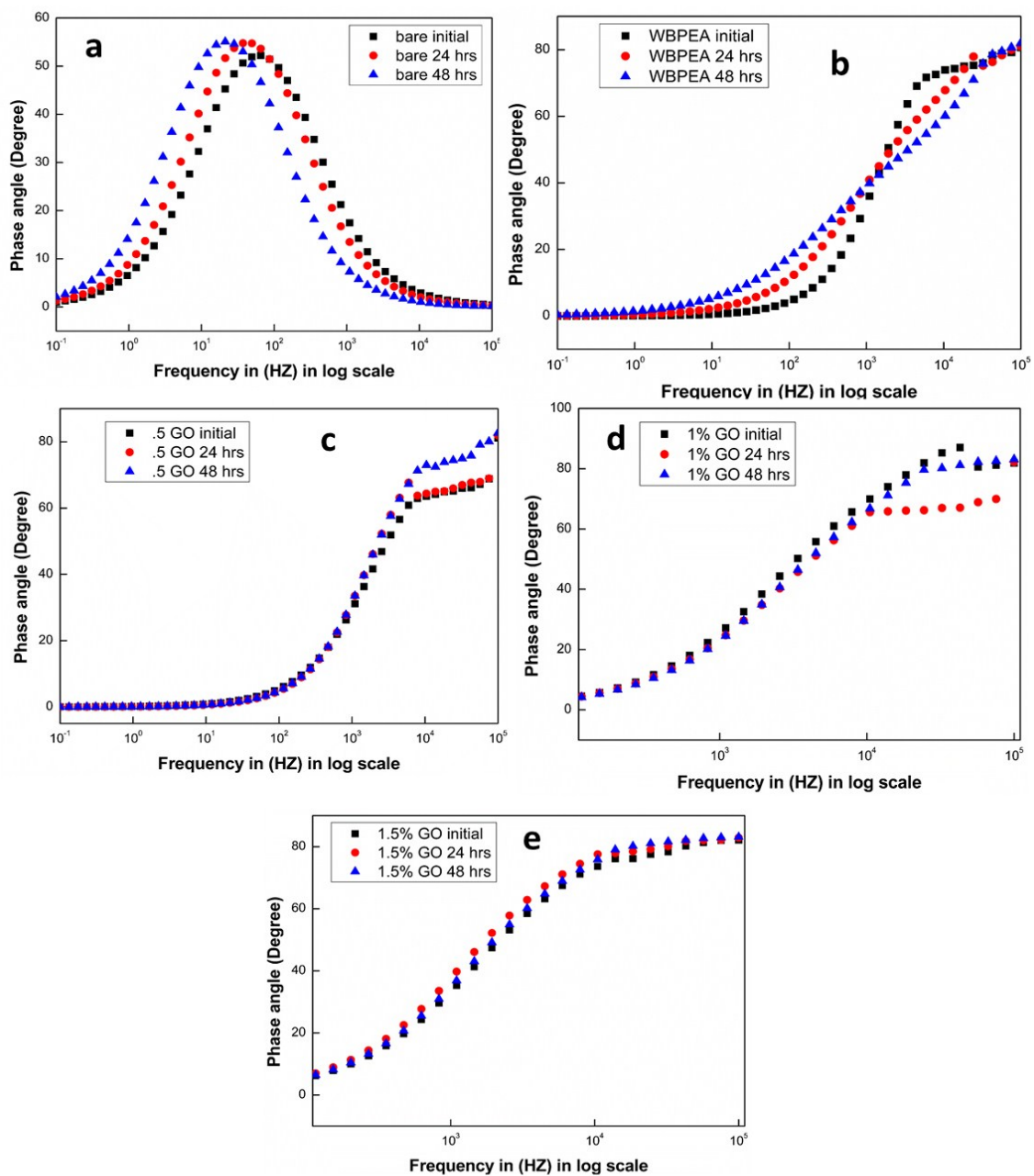


**Fig. S7.** Phase angle variation in pH 4 (a) bare CS (b) WBPEA-PMF-80 (c) WBPEA-PMF-80-RGO-0.5 (d) WBPEA-PMF-80-RGO-1.0 (e) WBPEA-PMF-80-RGO-1.5.

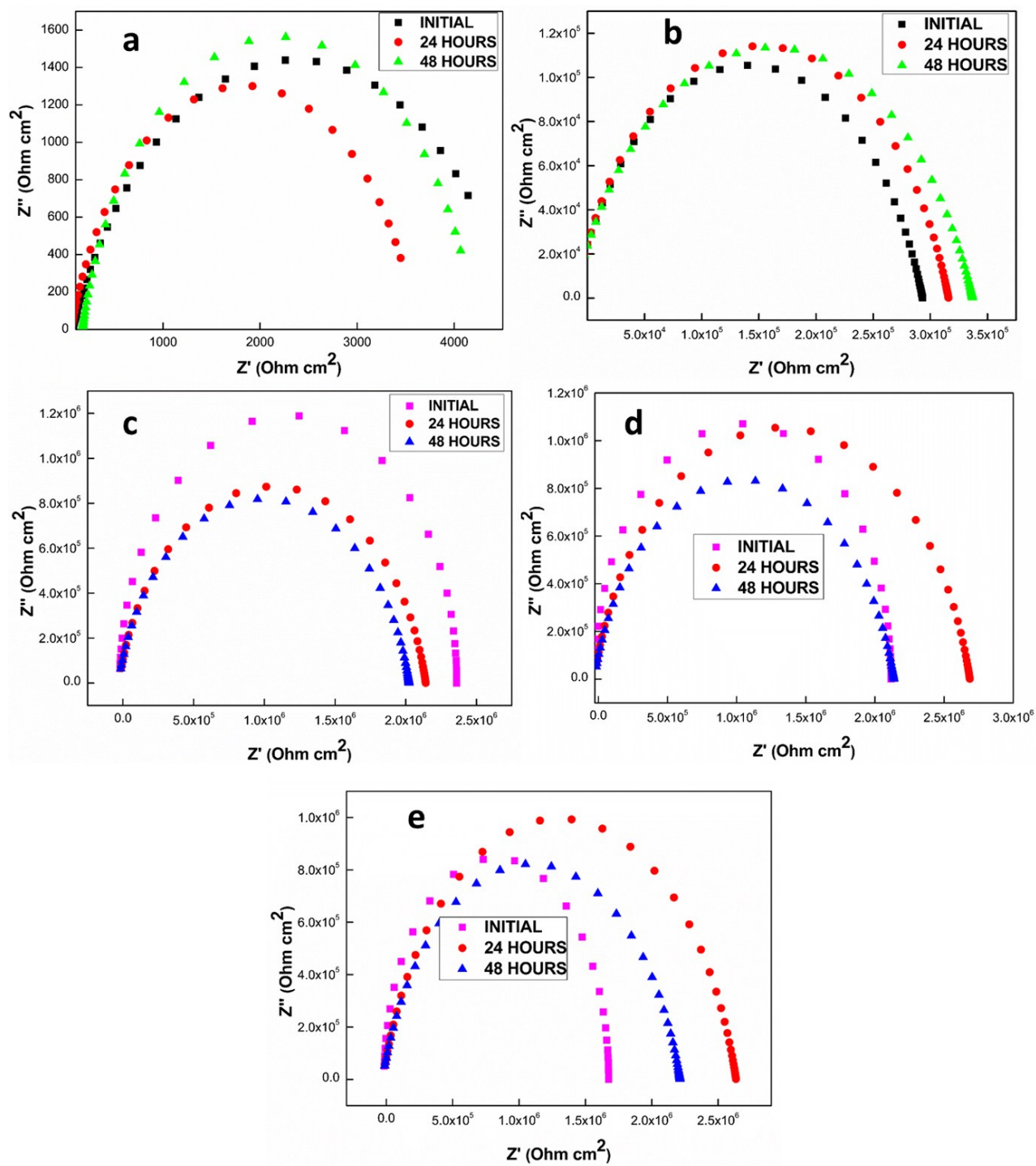


**Fig. S8.** Nyquist plots in pH 7 (a) bare CS (b) WBPEA-PMF-80 (c) WBPEA-PMF-80-RGO-0.5 (d) WBPEA-PMF-80-RGO-1.0 (e) WBPEA-PMF-80-RGO-1.5.

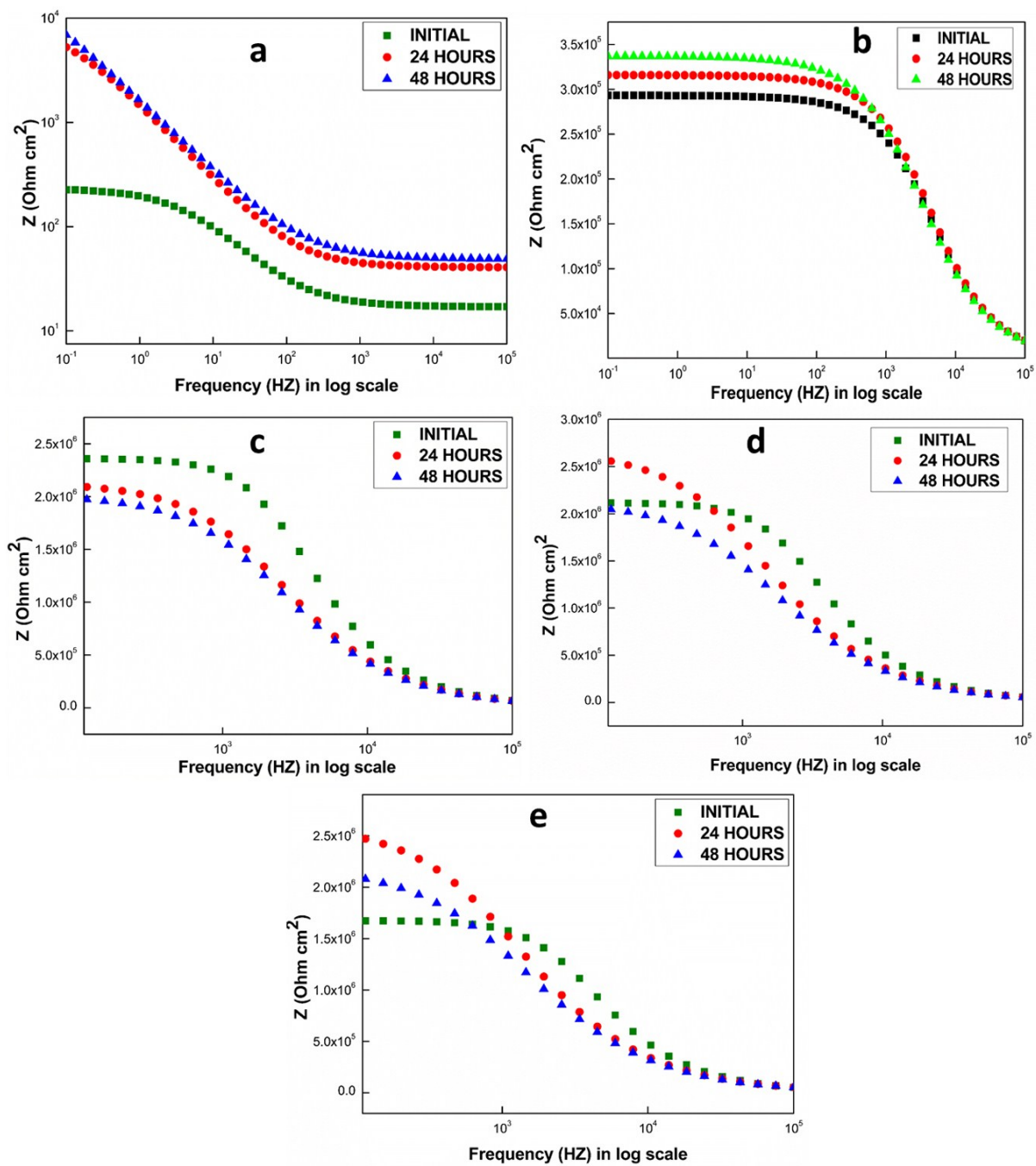


**Fig. S9.** Bode plots in pH 7 (a) bare CS (b) WBPEA-PMF-80 (c) WBPEA-PMF-80-RGO-0.5 (d) WBPEA-PMF-80-RGO-1.0 (e) WBPEA-PMF-80-RGO-1.5.

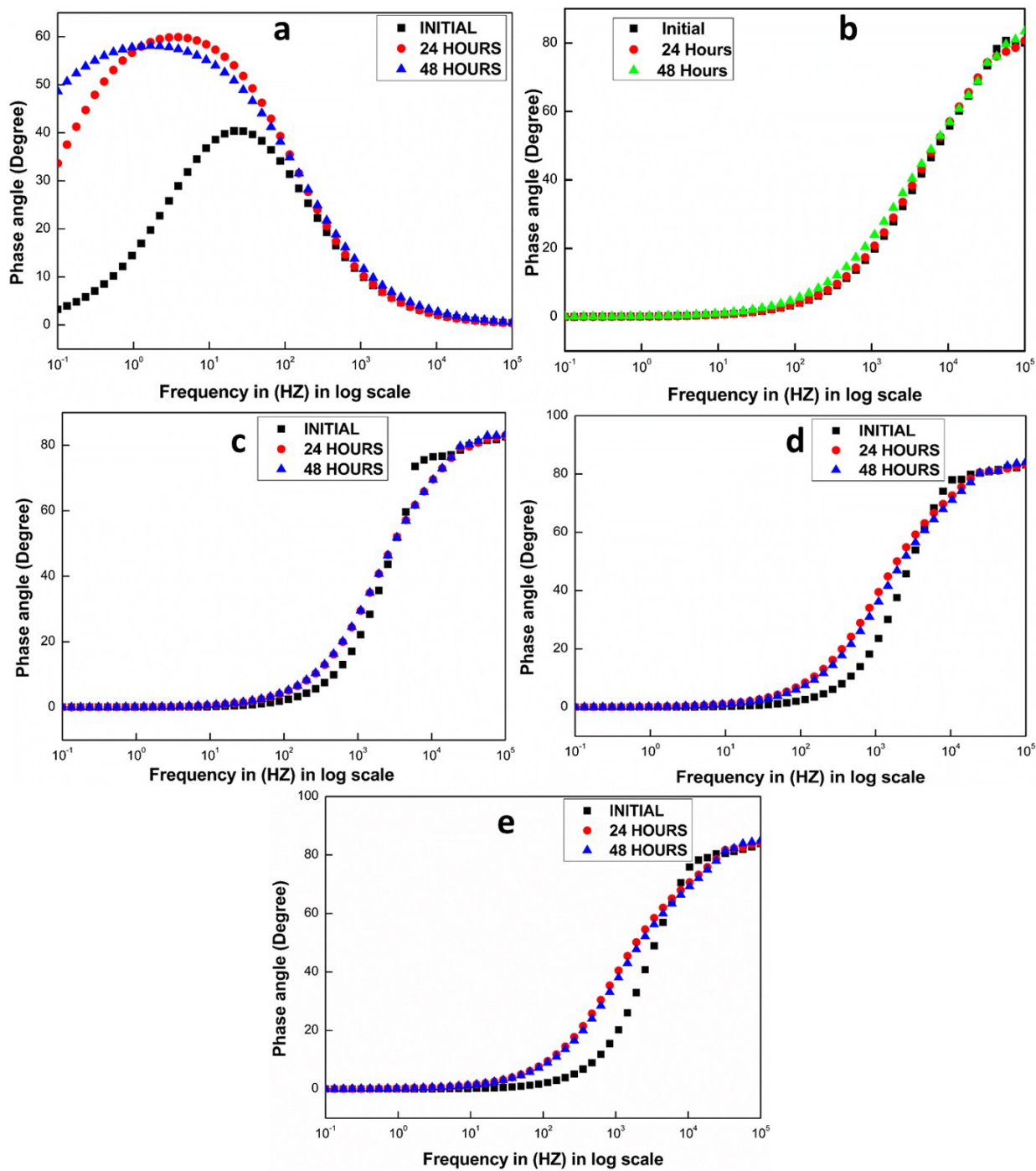


**Fig. S10.** Phase angle variation in pH 7 (a) bare CS (b) WBPEA-PMF-80 (c) WBPEA-PMF-80-RGO-0.5 (d) WBPEA-PMF-80-RGO-1.0 (e) WBPEA-PMF-80-RGO-1.5.

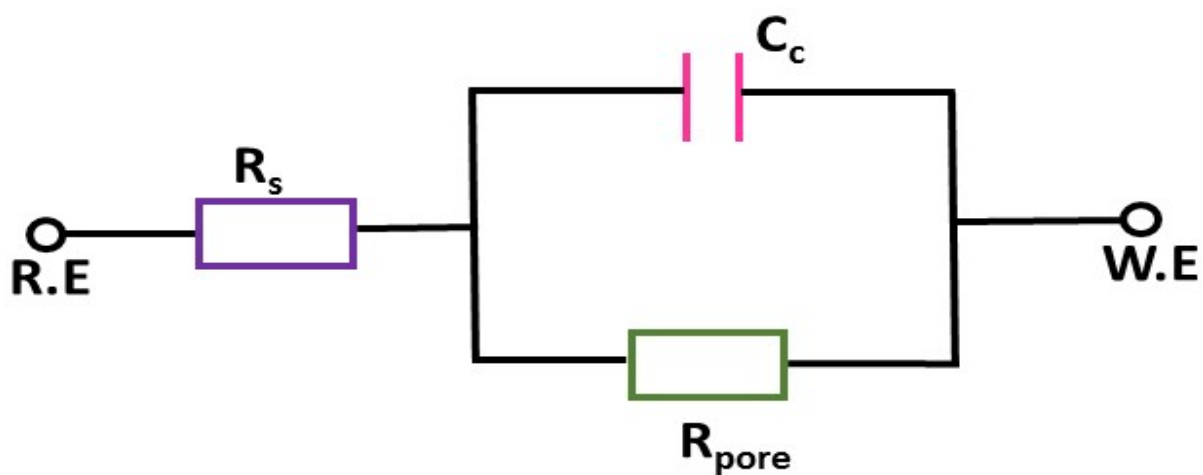


**Fig. S11.** Equivalent fitted circuits used in EIS.

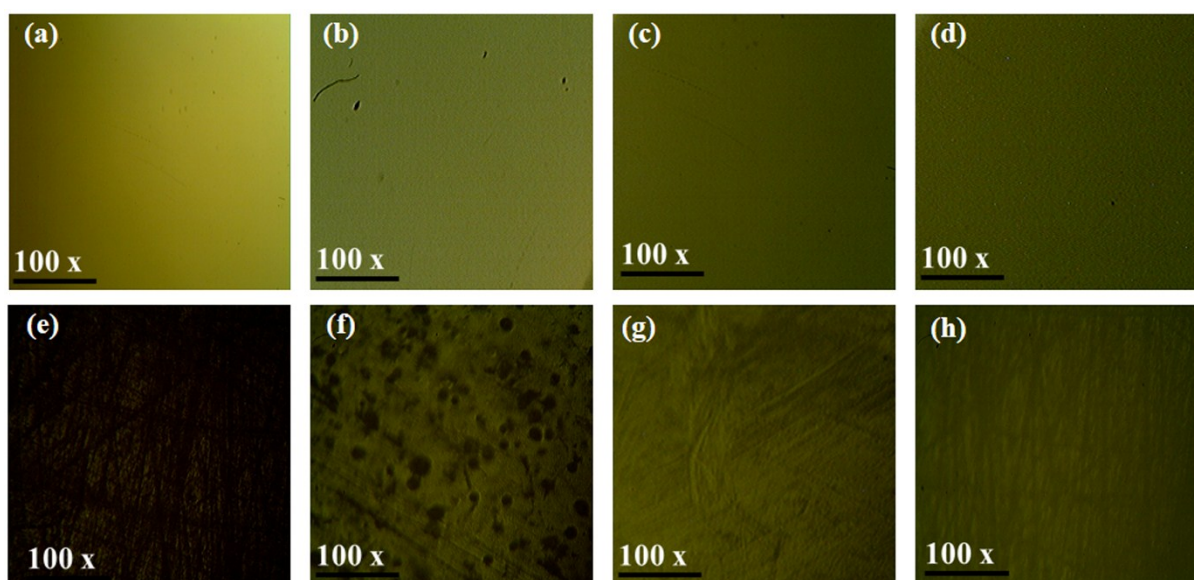


**Fig. S12.** Optical micrograph of (a, e) WBPEA-PMF-80 (b, f) WBPEA-PMF-80-RGO-0.5 (c, g) WBPEA-PMF-80-RGO-1.0 (g, h) WBPEA-PMF-80-RGO-1.5 before and after corrosion studies.

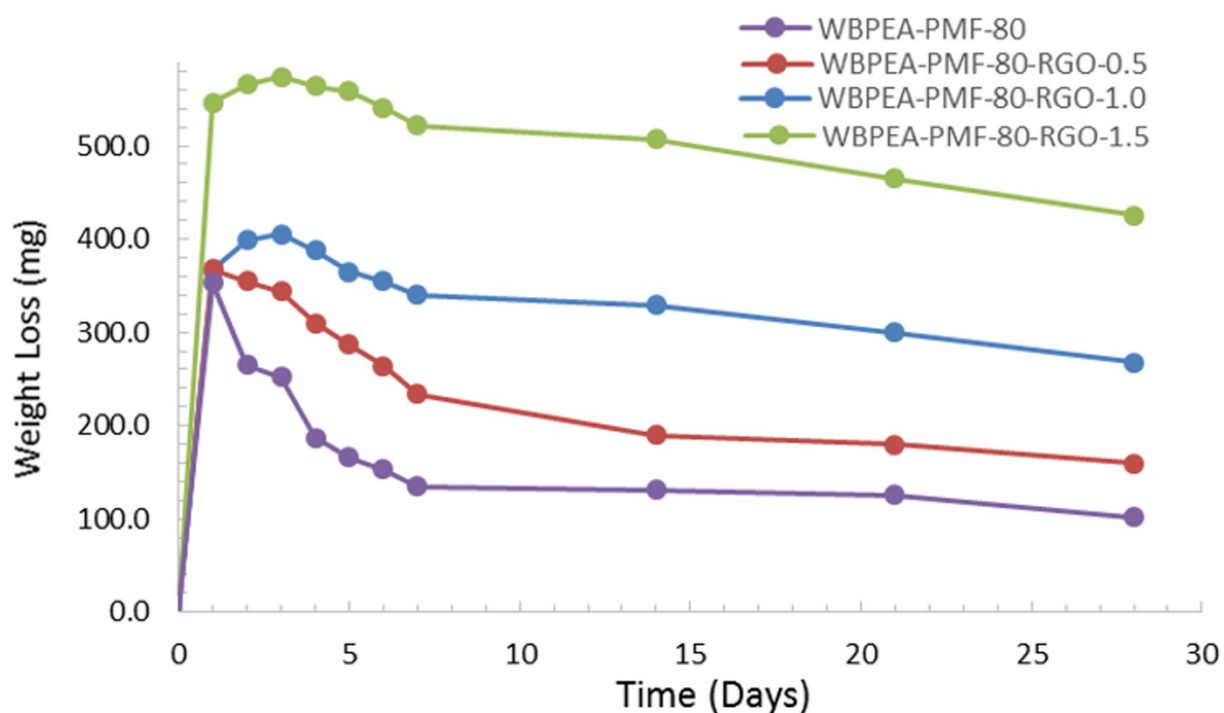


**Fig. S13.** Degradation of WBPEA-PMF-80, WBPEA-PMF-80-RGO-0.5, WBPEA-PMF-80-RGO-1.0 and WBPEA-PMF-80-RGO-1.5 for 28 days.

**Table S1. Physico-chemical properties**

Resin code	Specific density	Refractive index	Viscosity (m.Pas)	Acid value
Soy oil	0.91136	1.471	43.8	-
HESA	0.95703	1.475	1315	-
WBPEA	1.03042	1.499	10086.15	40
WBPEA-PMF-80	1.1063	1.51	12400.20	-
WBPEA-PMF-80-RGO-0.5	1.1098	1.59	12405.10	-
WBPEA-PMF-80-RGO-1	1.1422	1.62	12411.35	-
WBPEA-PMF-80-RGO-1.5	1.1589	1.65	12421.30	-

**Table S2. Physico-mechanical properties**

Resin Code	WBPEA- PMF-80	WBPEA-PMF- 80-RGO-0.5	WBPEA-PMF- 80-RGO-1.5
Gloss at 45°	62	59	45
Scratch hardness (kg)	4.832	8.18	11.5
Impact resistance (150 lb/inch)	fail	pass	pass
Cross hatch test	Pass	Pass	pass
Bending (1/8 inch)	pass	pass	pass
Dry time (min)	45	35	30
MEK test	>350	>350	>350
Coating thickness (µm)	92	95	97

**Table S3. Elemental analysis of GO and RGO**

Sample code	C Wt. %	N Wt. %	H Wt. %	O Wt. %
GO	15.65	0.00	0.790	23.571
RGO	66.15	1.32	2.016	11.620

**REFERENCES:**

- 1) S. Ahmad, S. M. Ashraf and F. Zafar, *Journal of Applied Polymer Science*, 2007, **104**, 1143–1148.
- 2) R. Justin and B. Chen, *J. Mater. Chem. B*, 2014, **2**, 3759-3770